

Exclusive photoproduction of a photon-meson pair: A new class of observables to probe GPDs

SPIN2023 conference

Saad Nabeebaccus
IJCLab



September 26, 2023

Based on 2212.00655, 2302.12026 and work in progress with S. Wallon, L. Szymanowski, B. Pire, G. Duplančić, K. Passek-Kumerički, J. Schönleber

Why consider a gamma-meson pair?

Understanding quark transversity

- Transverse spin content of the proton:

$$\begin{array}{ccc} |\uparrow\rangle_{(x)} & \sim & |\rightarrow\rangle + |\leftarrow\rangle \\ |\downarrow\rangle_{(x)} & \sim & |\rightarrow\rangle - |\leftarrow\rangle \\ \text{spin along } x & & \text{helicity states} \end{array}$$

- Observables which are sensitive to helicity flip thus give access to transversity PDFs. Poorly known.

Why consider a gamma-meson pair?

Understanding quark transversity

- Transverse spin content of the proton:

$$\begin{array}{ccc} |\uparrow\rangle_{(x)} & \sim & |\rightarrow\rangle + |\leftarrow\rangle \\ |\downarrow\rangle_{(x)} & \sim & |\rightarrow\rangle - |\leftarrow\rangle \\ \text{spin along } x & & \text{helicity states} \end{array}$$

- Observables which are sensitive to helicity flip thus give access to transversity PDFs. Poorly known.
- Transversity GPDs are completely unknown experimentally.

Why consider a gamma-meson pair?

Understanding quark transversity

- ▶ Transverse spin content of the proton:

$$\begin{array}{ccc} |\uparrow\rangle_{(x)} & \sim & |\rightarrow\rangle + |\leftarrow\rangle \\ |\downarrow\rangle_{(x)} & \sim & |\rightarrow\rangle - |\leftarrow\rangle \\ \text{spin along } x & & \text{helicity states} \end{array}$$

- ▶ Observables which are sensitive to helicity flip thus give access to transversity PDFs. Poorly known.
- ▶ Transversity GPDs are completely unknown experimentally.
- ▶ For massless (anti)particles, chirality = (-)helicity
- ▶ Transversity GPDs can thus be accessed through **chiral-odd** Γ matrices.

Why consider a gamma-meson pair?

Understanding quark transversity

- ▶ Transverse spin content of the proton:

$$\begin{array}{ll} |\uparrow\rangle_{(x)} & \sim |\rightarrow\rangle + |\leftarrow\rangle \\ |\downarrow\rangle_{(x)} & \sim |\rightarrow\rangle - |\leftarrow\rangle \end{array}$$

spin along x helicity states

- ▶ Observables which are sensitive to helicity flip thus give access to transversity PDFs. Poorly known.
- ▶ Transversity GPDs are completely unknown experimentally.
- ▶ For massless (anti)particles, chirality = (-)helicity
- ▶ Transversity GPDs can thus be accessed through **chiral-odd Γ matrices**.
- ▶ Since (in the massless limit) QCD and QED are chiral-even $(\gamma^\mu, \gamma^\mu\gamma^5)$, **the chiral-odd quantities $(1, \gamma^5, [\gamma^\mu, \gamma^\nu])$ which one wants to measure should appear in pairs.**

Why consider a gamma-meson pair?

Can we probe quark transversity GPDs in DVMP?

- ▶ the leading DA (twist 2) of ρ_T is **chiral-odd** ($\sigma^{\mu\nu}$ coupling)

Why consider a gamma-meson pair?

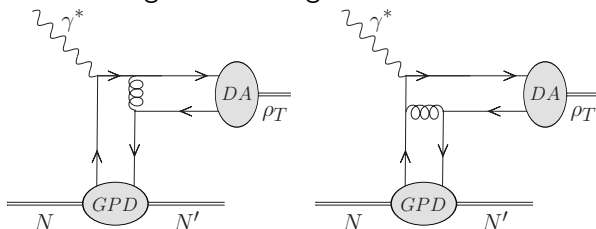
Can we probe quark transversity GPDs in DVMP?

- ▶ the leading DA (twist 2) of ρ_T is **chiral-odd** ($\sigma^{\mu\nu}$ coupling)
- ▶ unfortunately $\gamma^* N \rightarrow \rho_T N' = 0$, since such a process would require a helicity transfer of 2 from a photon. [M. Diehl, T. Gousset, B. Pire: hep-ph/9808479], [J. Collins, M. Diehl: hep-ph/9907498]

Why consider a gamma-meson pair?

Can we probe quark transversity GPDs in DVMP?

- ▶ the leading DA (twist 2) of ρ_T is **chiral-odd** ($\sigma^{\mu\nu}$ coupling)
- ▶ unfortunately $\gamma^* N \rightarrow \rho_T N' = 0$, since such a process would require a helicity transfer of 2 from a photon. [M. Diehl, T. Gousset, B. Pire: hep-ph/9808479], [J. Collins, M. Diehl: hep-ph/9907498]
- ▶ lowest order diagrammatic argument:



$$\gamma^\alpha [\gamma^\mu, \gamma^\nu] \gamma_\alpha = 0$$

Why consider a gamma-meson pair?

A convenient solution

Circumvent this using 3-body final states:

► $\gamma N \rightarrow MMN'$:

M. El Beiyad, R. Enberg, D. Ivanov, B. Pire, M. Segond, L. Szymanowski,
O. Teryaev, S. Wallon: [hep-ph/0209300, hep-ph/0601138, 1001.4491]

► $\gamma N \rightarrow \gamma MN'$:

R. Boussarie, G. Duplančić, **S.N.**, K. Passek-Kumerički, B. Pire,
L. Szymanowski, S. Wallon: [1609.03830, 1809.08104, 2212.00655, 2302.12026]

Why consider a gamma-meson pair?

A convenient solution

Circumvent this using 3-body final states:

► $\gamma N \rightarrow MMN'$:

M. El Beiyad, R. Enberg, D. Ivanov, B. Pire, M. Segond, L. Szymanowski,
O. Teryaev, S. Wallon: [hep-ph/0209300, hep-ph/0601138, 1001.4491]

► $\gamma N \rightarrow \gamma MN'$:

R. Boussarie, G. Duplančić, **S.N.**, K. Passek-Kumerički, B. Pire,
L. Szymanowski, S. Wallon: [1609.03830, 1809.08104, 2212.00655, 2302.12026]

Moreover, the richer kinematics of the process allows the sensitivity of GPDs wrt x to be probed (beyond moment-type dependence, e.g. in DVCS) J. Qiu, Z. Yu: [2305.15397]

Why consider a gamma-meson pair?

A convenient solution

Circumvent this using 3-body final states:

► $\gamma N \rightarrow MMN'$:

M. El Beiyad, R. Enberg, D. Ivanov, B. Pire, M. Segond, L. Szymanowski,
O. Teryaev, S. Wallon: [hep-ph/0209300, hep-ph/0601138, 1001.4491]

► $\gamma N \rightarrow \gamma MN'$:

R. Boussarie, G. Duplančić, **S.N.**, K. Passek-Kumerički, B. Pire,
L. Szymanowski, S. Wallon: [1609.03830, 1809.08104, 2212.00655, 2302.12026]

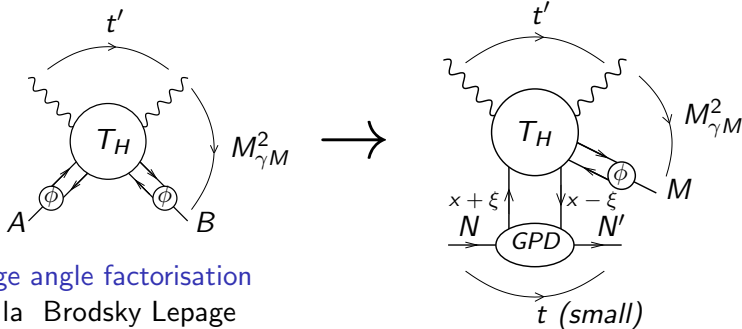
Moreover, the richer kinematics of the process allows the sensitivity of GPDs wrt x to be probed (beyond moment-type dependence, e.g. in DVCS) J. Qiu, Z. Yu: [2305.15397]

Also many others that are not sensitive to chiral-odd GPDs, such as DDVCS: *See talks by Victor and Marie*

Why consider a gamma-meson pair?

A convenient solution

- Consider the process $\gamma N \rightarrow \gamma M N'$, $M = \text{meson}$. Collinear factorisation of the amplitude at large $M_{\gamma M}^2$, t' , u' , and small t .

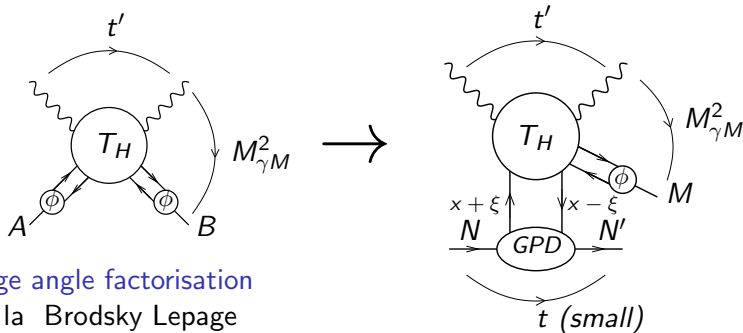


large angle factorisation
à la Brodsky Lepage

Why consider a gamma-meson pair?

A convenient solution

- Consider the process $\gamma N \rightarrow \gamma M N'$, $M = \text{meson}$. Collinear factorisation of the amplitude at large $M_{\gamma M}^2$, t' , u' , and small t .



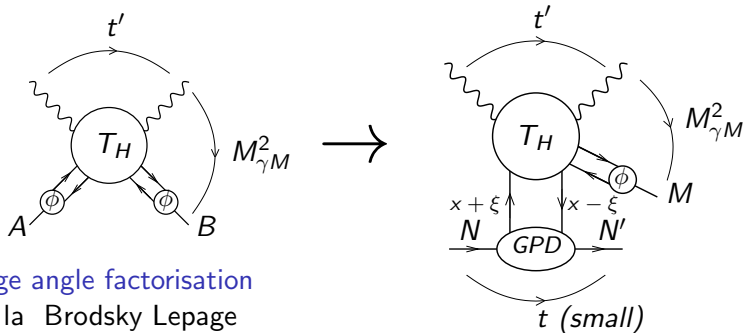
large angle factorisation
à la Brodsky Lepage

- Mesons considered in the final state: $\pi^{\pm}, \rho_{L,T}^{\pm,0}$.

Why consider a gamma-meson pair?

A convenient solution

- Consider the process $\gamma N \rightarrow \gamma M N'$, $M = \text{meson}$. Collinear factorisation of the amplitude at large $M_{\gamma M}^2$, t' , u' , and small t .



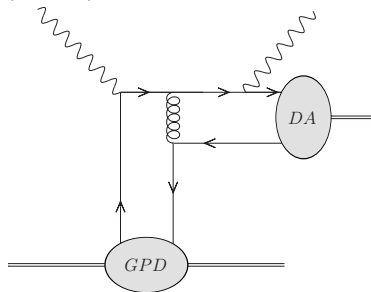
large angle factorisation
à la Brodsky Lepage

- Mesons considered in the final state: π^{\pm} , $\rho_{L,T}^{\pm,0}$.
- Leading order and leading twist

Why consider a gamma-meson pair?

Chiral-odd GPDs using $\rho_T \gamma$ production

How does it work (at LO)?

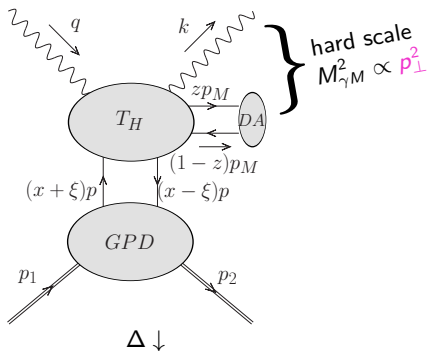


Typical non-zero diagram for a **transverse** ρ meson

the σ matrices (from either the DA or the GPD) do not kill it anymore!

Kinematics

$$\gamma(q) + N(p_1) \rightarrow \gamma(k) + M(p_M, \varepsilon_M) + N'(p_2)$$



Useful Mandelstam variables:

$$t = (p_2 - p_1)^2,$$

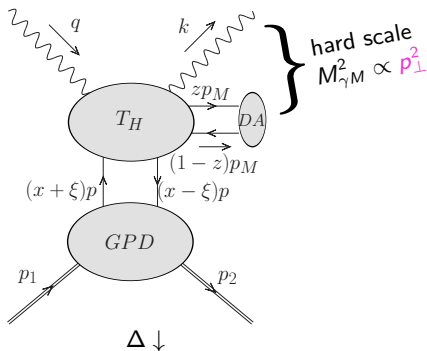
$$u' = (p_M - q)^2,$$

$$t' = (k - q)^2,$$

$$S_{\gamma N} = (q + p_1)^2 \; .$$

- Factorisation requires:
 $-u' > 1 \text{ GeV}^2$, $-t' > 1 \text{ GeV}^2$ and $(-t)_{\min} \leq -t \leq .5 \text{ GeV}^2$
 \Rightarrow sufficient to ensure large p_T .

$$\gamma(q) + N(p_1) \rightarrow \gamma(k) + M(p_M, \varepsilon_M) + N'(p_2)$$



Useful Mandelstam variables:

$$t = (p_2 - p_1)^2,$$

$$u' = (p_M - q)^2,$$

$$t' = (k - q)^2,$$

$$S_{\gamma N} = (q + p_1)^2.$$

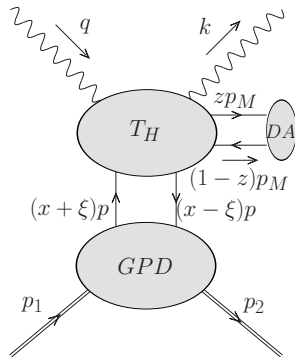
- Factorisation requires:
 $-u' > 1 \text{ GeV}^2$, $-t' > 1 \text{ GeV}^2$ and $(-t)_{\min} \leq -t \leq .5 \text{ GeV}^2$
 \implies sufficient to ensure **large** p_T .
- Cross-section differential in $(-u')$ and $M_{\gamma M}^2$, and evaluated at $(-t) = (-t)_{\min}$, covering $S_{\gamma N}$ from $\sim 4 \text{ GeV}^2$ to 20000 GeV^2 .

$$\mathcal{A} = \int_{-1}^1 dx \int_0^1 dz \, T(x, \xi, z) \, H(x, \xi, t) \, \Phi_M(z)$$

$$\mathcal{A} = \int_{-1}^1 dx \int_0^1 dz \, T(x, \xi, z) \, H(x, \xi, t) \, \Phi_M(z)$$

► Differential cross section:

$$\left. \frac{d\sigma}{dt \, du' \, dM_{\gamma M}^2} \right|_{-t=(-t)_{min}} = \frac{|\overline{\mathcal{A}}|^2}{32 S_{\gamma N}^2 M_{\gamma M}^2 (2\pi)^3}.$$



$$\mathcal{A} = \int_{-1}^1 dx \int_0^1 dz T(x, \xi, z) H(x, \xi, t) \Phi_M(z)$$

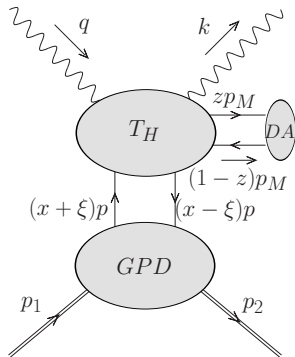
- Differential cross section:

$$\left. \frac{d\sigma}{dt du' dM_{\gamma M}^2} \right|_{-t=(-t)_{min}} = \frac{|\overline{\mathcal{A}}|^2}{32 S_{\gamma N}^2 M_{\gamma M}^2 (2\pi)^3}.$$

- Kinematic parameters: $S_{\gamma N}$, $M_{\gamma M}^2$, $-t$, $-u'$
- Useful dimensionless variables (hard part):

$$\alpha = \frac{-u'}{M_{\gamma M}^2},$$

$$\xi = \frac{M_{\gamma M}^2}{2(S_{\gamma N} - m_N^2) - M_{\gamma M}^2}.$$



Quark GPDs are parametrised in terms of **Double Distributions**
[A. Radyushkin: [hep-ph/9805342](#)]

Quark GPDs are parametrised in terms of **Double Distributions**
[A. Radyushkin: [hep-ph/9805342](#)]

For **polarised** PDFs (and hence **transversity** PDFs), two scenarios are proposed for the parameterization:

- ▶ “**standard**” scenario, with flavor-symmetric light sea quark and antiquark distributions.
- ▶ “**valence**” scenario with a completely flavor-asymmetric light sea quark densities.

- We take the simplistic **asymptotic** form of the DAs

$$\phi_{\text{as}}(z) = 6z(1 - z) .$$

- ▶ We take the simplistic **asymptotic** form of the DAs

$$\phi_{\text{as}}(z) = 6z(1 - z).$$

- ▶ We also investigate the effect of using a **holographic** DA:

$$\phi_{\text{hol}}(z) = \frac{8}{\pi} \sqrt{z(1 - z)}.$$

Suggested by

- ▶ AdS/QCD correspondence [S. Brodsky, G. de Teramond: [hep-ph/0602252](#)],
- ▶ dynamical chiral symmetry breaking on the light-front [C. Shi, C. Chen, L. Chang, C. Roberts, S. Schmidt, H. Zong: [1504.00689](#)],
- ▶ recent lattice results. [X. Gao, A. Hanlon, N. Karthik, S. Mukherjee, P. Petreczky, P. Scior, S. Syritsyn, Y. Zhao: [2206.04084](#)]

Is QCD collinear factorisation really justified?

- ▶ Recently, factorisation has been proved for the process $\pi^\pm N \rightarrow \gamma\gamma N'$ by J. Qiu, Z. Yu [2205.07846].
- ▶ This was extended to a wide range of $2 \rightarrow 3$ exclusive processes by J. Qiu, Z. Yu [2210.07995]

Is QCD collinear factorisation really justified?

- ▶ Recently, factorisation has been proved for the process $\pi^\pm N \rightarrow \gamma\gamma N'$ by J. Qiu, Z. Yu [2205.07846].
- ▶ This was extended to a wide range of $2 \rightarrow 3$ exclusive processes by J. Qiu, Z. Yu [2210.07995]
- ▶ The proof relies on having large p_T , rather than large invariant mass (e.g. photon-meson pair).

Is QCD collinear factorisation really justified?

- ▶ Recently, factorisation has been proved for the process $\pi^\pm N \rightarrow \gamma\gamma N'$ by J. Qiu, Z. Yu [2205.07846].
- ▶ This was extended to a wide range of $2 \rightarrow 3$ exclusive processes by J. Qiu, Z. Yu [2210.07995]
- ▶ The proof relies on having large p_T , rather than large invariant mass (e.g. photon-meson pair).
- ▶ In fact, NLO computation has been performed for $\gamma N \rightarrow \gamma\gamma N'$ by O. Grocholski, B. Pire, P. Sznajder, L. Szymanowski, J. Wagner [2110.00048]
- ▶ Also, NLO computation for $\gamma\gamma \rightarrow \pi^+\pi^-$ by crossing symmetry G. Duplancic, B. Nizic: [hep-ph/0607069].

Exclusive photoproduction of $\pi^0\gamma$

Gluonic GPD contributions

- Because of the quantum numbers of π^0 ($J^{PC} = 0^{-+}$), the exclusive photoproduction of $\pi^0\gamma$ is also sensitive to gluonic GPD contributions.

Exclusive photoproduction of $\pi^0\gamma$

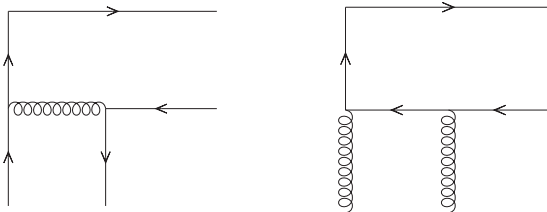
Gluonic GPD contributions

- ▶ Because of the quantum numbers of π^0 ($J^{PC} = 0^{-+}$), the exclusive photoproduction of $\pi^0\gamma$ is also sensitive to gluonic GPD contributions.
- ▶ A total of 24 diagrams contribute in this case (compared to 20 diagrams from quark GPD contributions), with 6 groups of 4 related by symmetries ($x \rightarrow -x$ and $z \rightarrow 1 - z$ separately).

Exclusive photoproduction of $\pi^0\gamma$

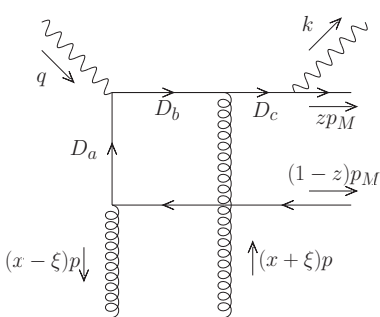
Gluonic GPD contributions

- ▶ Because of the quantum numbers of π^0 ($J^{PC} = 0^{-+}$), the exclusive photoproduction of $\pi^0\gamma$ is also sensitive to gluonic GPD contributions.
- ▶ A total of 24 diagrams contribute in this case (compared to 20 diagrams from quark GPD contributions), with 6 groups of 4 related by symmetries ($x \rightarrow -x$ and $z \rightarrow 1 - z$ separately).
- ▶ Diagrams amount to connecting photons to the following two topologies.



Exclusive photoproduction of $\pi^0\gamma$

Gluonic GPD contributions



$$D_a = ((x - \xi)p + \bar{z}p_M)^2 + i\epsilon$$

$$= s\bar{\alpha}\bar{z} \left[x - \xi + i\epsilon \right] ,$$

$$D_b = (k + zp_M - (x + \xi)p)^2 + i\epsilon$$

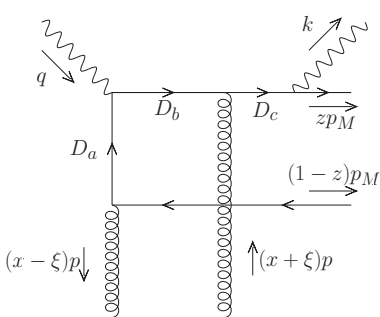
$$= -s \left[z \left(x - \xi - i\epsilon \right) + \alpha\bar{z} (x + \xi - i\epsilon) \right] ,$$

$$D_c = (k + zp_M)^2 + i\epsilon$$

$$= 2s\xi z + i\epsilon$$

Exclusive photoproduction of $\pi^0\gamma$

Gluonic GPD contributions



$$D_a = ((x - \xi)p + \bar{z}p_M)^2 + i\epsilon$$

$$= s\bar{\alpha}\bar{z} \left[x - \xi + i\epsilon \right] ,$$

$$D_b = (k + zp_M - (x + \xi)p)^2 + i\epsilon$$

$$= -s \left[z \left(x - \xi - i\epsilon \right) + \alpha\bar{z} (x + \xi - i\epsilon) \right] ,$$

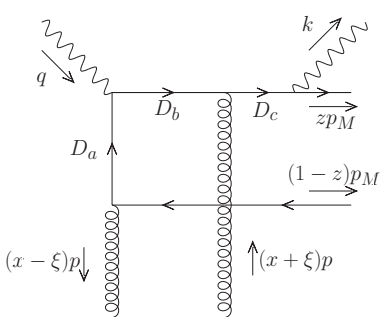
$$D_c = (k + zp_M)^2 + i\epsilon$$

$$= 2s\xi z + i\epsilon$$

\Rightarrow pinching of poles in the propagators in the limit of $z \rightarrow 1$

Exclusive photoproduction of $\pi^0\gamma$

Gluonic GPD contributions



$$D_a = ((x - \xi)p + \bar{z}p_M)^2 + i\epsilon$$

$$= s\bar{\alpha}\bar{z} \left[\boxed{x - \xi + i\epsilon} \right],$$

$$D_b = (k + zp_M - (x + \xi)p)^2 + i\epsilon$$

$$= -s \left[z \left(\boxed{x - \xi - i\epsilon} \right) + \alpha\bar{z}(x + \xi - i\epsilon) \right],$$

$$D_c = (k + zp_M)^2 + i\epsilon$$

$$= 2s\xi z + i\epsilon$$

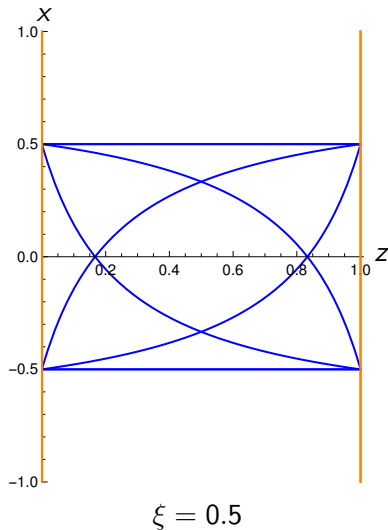
\Rightarrow *pinching of poles in the propagators in the limit of $z \rightarrow 1$*

Assuming an asymptotic form of the DA, they manifest themselves *as a purely imaginary part*, in terms of

- ▶ $\int_0^1 \frac{dz}{z\bar{z}}$ contributions, when the x -integration is performed first,
- ▶ $\int_1^1 dx \frac{\ln(x-\xi-i\epsilon)}{(x-\xi+i\epsilon)}$ contributions, when the z -integration is performed first.

Exclusive photoproduction of $\pi^0\gamma$

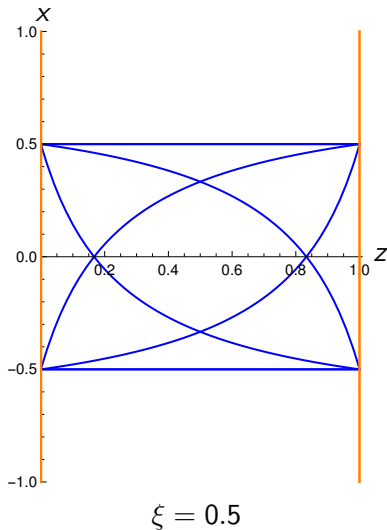
Gluonic GPD contributions: Singularity structure of the full amplitude



- Unfortunately, no cancellations between the 4 corners.

Exclusive photoproduction of $\pi^0\gamma$

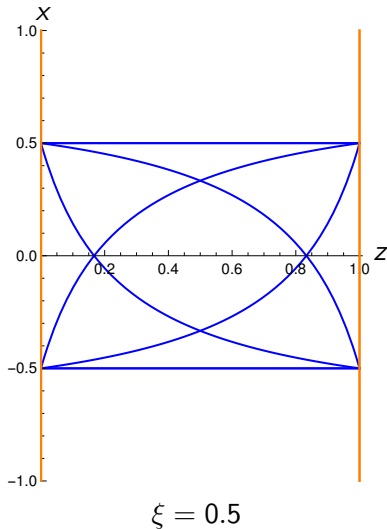
Gluonic GPD contributions: Singularity structure of the full amplitude



- Unfortunately, no cancellations between the 4 corners.
- Problem also shows up in $\pi^0 N \rightarrow \gamma\gamma N$.

Exclusive photoproduction of $\pi^0\gamma$

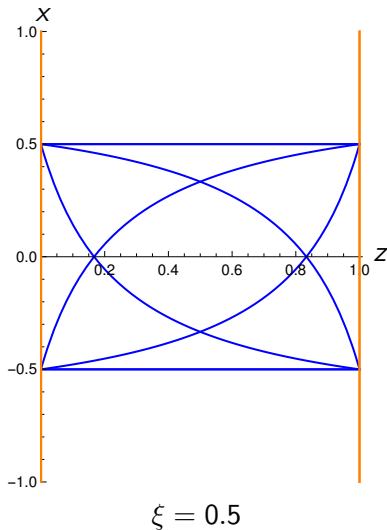
Gluonic GPD contributions: Singularity structure of the full amplitude



- ▶ Unfortunately, no cancellations between the 4 corners.
- ▶ Problem also shows up in $\pi^0 N \rightarrow \gamma\gamma N$.
- ▶ In $\gamma\gamma \rightarrow \pi^+\pi^-$, only ERBL region exists, no poles are crossed, and endpoint contributions are suppressed by DAs.

Exclusive photoproduction of $\pi^0\gamma$

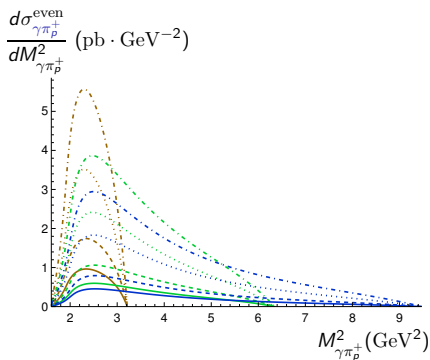
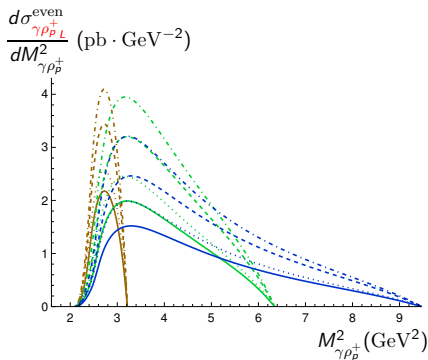
Gluonic GPD contributions: Singularity structure of the full amplitude



- ▶ Unfortunately, no cancellations between the 4 corners.
- ▶ Problem also shows up in $\pi^0 N \rightarrow \gamma\gamma N$.
- ▶ In $\gamma\gamma \rightarrow \pi^+\pi^-$, only ERBL region exists, no poles are crossed, and endpoint contributions are suppressed by DAs.
- ▶ Problem with factorisation? At twist-2??

Results

Single differential cross-section: $\gamma\rho_p^+$ vs $\gamma\pi_p^+$



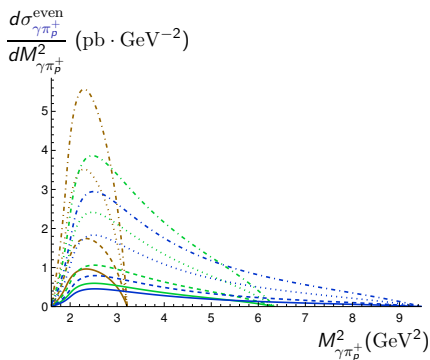
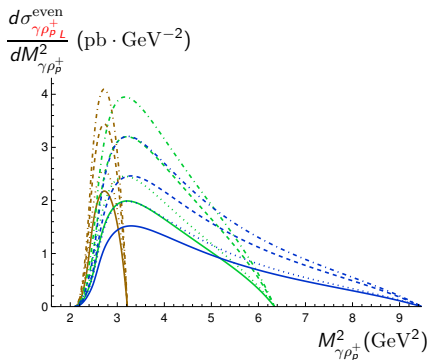
$$S_{\gamma N} = 8, 14, 20 \text{ GeV}^2$$

Dashed: Holographic DA non-dashed: Asymptotical DA

Dotted: standard scenario non-dotted: valence scenario

Results

Single differential cross-section: $\gamma\rho_p^+$ vs $\gamma\pi_p^+$



$$S_{\gamma N} = 8, 14, 20 \text{ GeV}^2$$

Dashed: Holographic DA non-dashed: Asymptotical DA

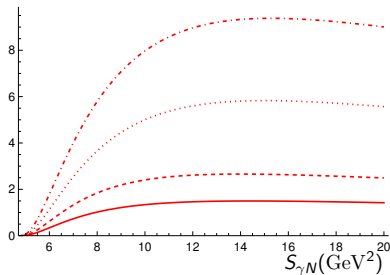
Dotted: standard scenario non-dotted: valence scenario

\Rightarrow Effect of GPD model more important on π_p^+ than on ρ_p^+

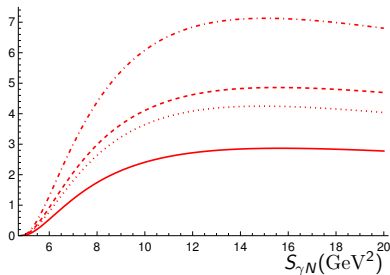
Results

Integrated cross-section: $\gamma\pi_p^+$ vs $\gamma\pi_n^-$

$\sigma_{\gamma\pi_p^+}^{even}$ (pb)



$\sigma_{\gamma\pi_n^-}^{even}$ (pb)



Dashed: Holographic DA

non-dashed: Asymptotical DA

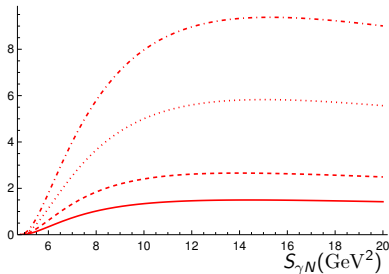
Dotted: standard scenario

non-dotted: valence scenario

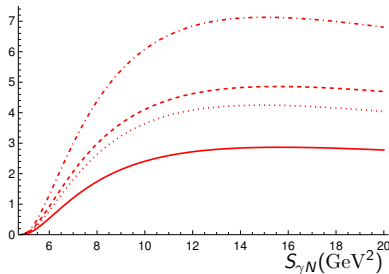
Results

Integrated cross-section: $\gamma\pi_p^+$ vs $\gamma\pi_n^-$

$\sigma_{\gamma\pi_p^+}^{even}$ (pb)



$\sigma_{\gamma\pi_n^-}^{even}$ (pb)



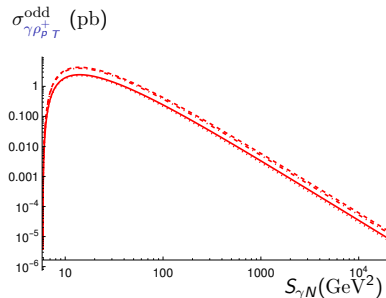
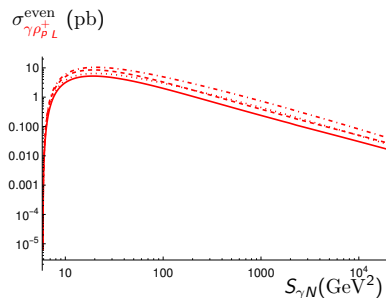
Dashed: Holographic DA non-dashed: Asymptotical DA

Dotted: standard scenario non-dotted: valence scenario

⇒ Huge effect from GPD model in π_p^+ case.

Results

Integrated cross-section: $\gamma\rho_{pL}^+$ vs $\gamma\rho_{pT}^+$



Dashed: Holographic DA

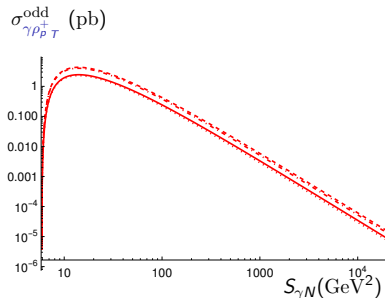
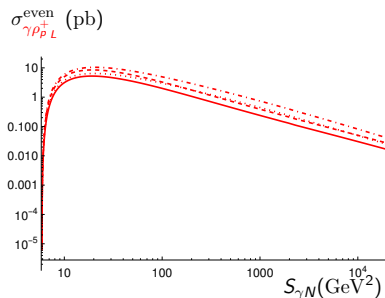
non-dashed: Asymptotical DA

Dotted: standard scenario

non-dotted: valence scenario

Results

Integrated cross-section: $\gamma\rho_{pL}^+$ vs $\gamma\rho_{pT}^+$



Dashed: Holographic DA non-dashed: Asymptotical DA

Dotted: standard scenario non-dotted: valence scenario

$\Rightarrow \xi^2$ suppression in the chiral-odd case causes the cross-section to drop rapidly with $S_{\gamma N}$ ($\xi \approx \frac{M_{\gamma\rho}^2}{2S_{\gamma N}}$).

Results

Polarisation Asymmetries wrt incoming photon

We consider an **unpolarised target**, and determine polarisation asymmetries wrt the incoming photon.

Results

Polarisation Asymmetries wrt incoming photon

We consider an **unpolarised target**, and determine polarisation asymmetries wrt the incoming photon.

- ▶ Circular polarisation asymmetry = 0.
- ▶ Linear polarisation asymmetry, $LPA = \frac{d\sigma_x - d\sigma_y}{d\sigma_x + d\sigma_y}$, where x is the direction defined by p_\perp (direction of outgoing photon in the transverse plane).

Results

Polarisation Asymmetries wrt incoming photon

We consider an **unpolarised target**, and determine polarisation asymmetries wrt the incoming photon.

- ▶ Circular polarisation asymmetry = 0.
- ▶ Linear polarisation asymmetry, $LPA = \frac{d\sigma_x - d\sigma_y}{d\sigma_x + d\sigma_y}$, where x is the direction defined by p_\perp (direction of outgoing photon in the transverse plane).
- ▶ In fact,

$$LPA_{\text{Lab}} = LPA \cos(2\theta) ,$$

where θ is the angle between the lab frame x -direction and p_\perp .

Results

Polarisation Asymmetries wrt incoming photon

We consider an **unpolarised target**, and determine polarisation asymmetries wrt the incoming photon.

- ▶ Circular polarisation asymmetry = 0.
- ▶ Linear polarisation asymmetry, $LPA = \frac{d\sigma_x - d\sigma_y}{d\sigma_x + d\sigma_y}$, where x is the direction defined by p_\perp (direction of outgoing photon in the transverse plane).

- ▶ In fact,

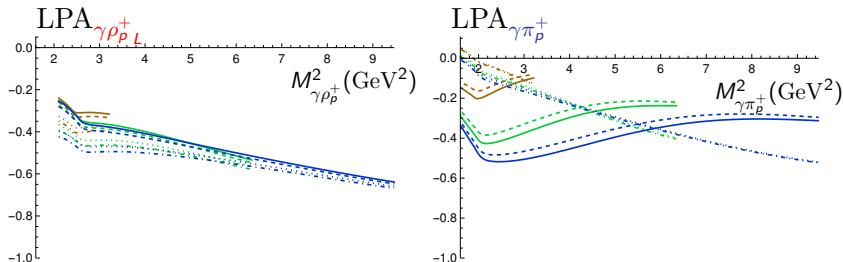
$$LPA_{\text{Lab}} = LPA \cos(2\theta) ,$$

where θ is the angle between the lab frame x -direction and p_\perp .

- ▶ **Kleiss-Sterling** spinor techniques used to obtain expressions.
- ▶ **Both asymmetries zero in chiral-odd case!**

Results

LPA wrt incoming photon: Single-differential level: $\gamma\rho_p^+$ vs $\gamma\pi_p^+$



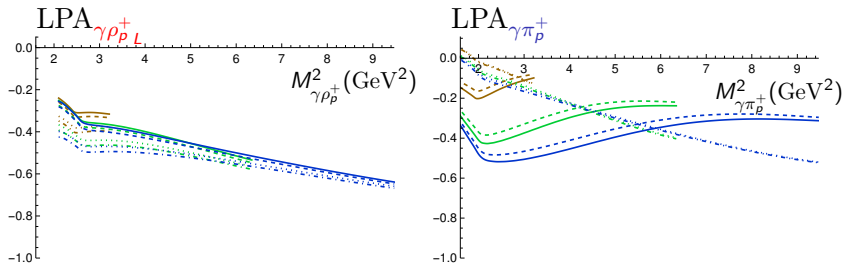
$$S_{\gamma N} = 8, 14, 20 \text{ GeV}^2$$

Dashed: Holographic DA non-dashed: Asymptotical DA

Dotted: standard scenario non-dotted: valence scenario

Results

LPA wrt incoming photon: Single-differential level: $\gamma\rho_p^+$ vs $\gamma\pi_p^+$



$$S_{\gamma N} = 8, 14, 20 \text{ GeV}^2$$

Dashed: Holographic DA non-dashed: Asymptotical DA

Dotted: standard scenario non-dotted: valence scenario

\Rightarrow GPD model changes the behaviour of the LPA completely in the π_p^+ case!

Prospects at experiments

Counting rates: JLab

Can be measured at JLab, COMPASS, future EIC and LHC (in UPCs)

Prospects at experiments

Counting rates: JLab

Can be measured at JLab, COMPASS, future EIC and LHC (in UPCs)

Good statistics: For example, at JLab Hall B:

- ▶ untagged incoming $\gamma \Rightarrow$ Weizsäcker-Williams distribution

Prospects at experiments

Counting rates: JLab

Can be measured at JLab, COMPASS, future EIC and LHC (in UPCs)

Good statistics: For example, at [JLab Hall B](#):

- ▶ untagged incoming $\gamma \Rightarrow$ **Weizsäcker-Williams** distribution
- ▶ with an expected luminosity of $\mathcal{L} = 100 \text{ nb}^{-1}\text{s}^{-1}$, for 100 days of run:
 - ρ_L^0 (on p) : $\approx 2.4 \times 10^5$
 - ρ_T^0 (on p) : $\approx 4.2 \times 10^4$ (Chiral-odd)
 - ρ_L^+ : $\approx 1.4 \times 10^5$
 - ρ_T^+ : $\approx 6.7 \times 10^4$ (Chiral-odd)
 - π^+ : $\approx 1.8 \times 10^5$

Prospects at experiments

Counting rates: JLab

Can be measured at JLab, COMPASS, future EIC and LHC (in UPCs)

Good statistics: For example, at [JLab Hall B](#):

- ▶ untagged incoming $\gamma \Rightarrow$ **Weizsäcker-Williams** distribution
- ▶ with an expected luminosity of $\mathcal{L} = 100 \text{ nb}^{-1}\text{s}^{-1}$, for 100 days of run:
 - ρ_L^0 (on p) : $\approx 2.4 \times 10^5$
 - ρ_T^0 (on p) : $\approx 4.2 \times 10^4$ (Chiral-odd)
 - ρ_L^+ : $\approx 1.4 \times 10^5$
 - ρ_T^+ : $\approx 6.7 \times 10^4$ (Chiral-odd)
 - π^+ : $\approx 1.8 \times 10^5$
- ▶ No problem in detecting outgoing photon at JLab.

Prospects at experiments

Counting rates: EIC

- ▶ At the future EIC, with an expected integrated luminosity of 10 fb^{-1} (about 100 times smaller than JLab):
 - ρ_L^0 (on p) : $\approx 2.4 \times 10^4$
 - ρ_T^0 (on p) : $\approx 2.4 \times 10^3$ (Chiral-odd)
 - ρ_L^+ : $\approx 1.5 \times 10^4$
 - ρ_T^+ : $\approx 4.2 \times 10^3$ (Chiral-odd)
 - π^+ : $\approx 1.3 \times 10^4$

Prospects at experiments

Counting rates: EIC

- At the future **EIC**, with an expected integrated luminosity of 10 fb^{-1} (about 100 times smaller than JLab):

- ρ_L^0 (on p) : $\approx 2.4 \times 10^4$
- ρ_T^0 (on p) : $\approx 2.4 \times 10^3$ (Chiral-odd)
- ρ_L^+ : $\approx 1.5 \times 10^4$
- ρ_T^+ : $\approx 4.2 \times 10^3$ (Chiral-odd)
- π^+ : $\approx 1.3 \times 10^4$

- **Small ξ study:**

$300 < S_{\gamma N} / \text{GeV}^2 < 20000$ ($5 \cdot 10^{-5} < \xi < 5 \cdot 10^{-3}$):

- ρ_L^0 (on p) : $\approx 1.2 \times 10^3$
- ρ_T^0 (on p) : ≈ 6.5 (Chiral-odd) (**tiny**)
- ρ_L^+ : $\approx 9.3 \times 10^2$
- π^+ : $\approx 5.0 \times 10^2$

Conclusion

- ▶ Exclusive photoproduction of photon-meson pair provides additional channel for **extracting GPDs**: Interesting effects from choice of different mesons.

Conclusion

- ▶ Exclusive photoproduction of photon-meson pair provides additional channel for **extracting GPDs**: Interesting effects from choice of different mesons.
- ▶ Especially interesting since it can probe **chiral-odd GPDs** at the leading twist, and provides **better sensitivity to x -dependence of GPDs**.

Conclusion

- ▶ Exclusive photoproduction of photon-meson pair provides additional channel for **extracting GPDs**: Interesting effects from choice of different mesons.
- ▶ Especially interesting since it can probe **chiral-odd GPDs** at the leading twist, and provides **better sensitivity to x -dependence of GPDs**.
- ▶ **Proof of factorisation** for this family of processes now available, but intriguing possible violation of collinear factorisation at twist-2 with **gluonic contributions to $\pi^0\gamma$ photoproduction**.

Conclusion

- ▶ Exclusive photoproduction of photon-meson pair provides additional channel for **extracting GPDs**: Interesting effects from choice of different mesons.
- ▶ Especially interesting since it can probe **chiral-odd GPDs** at the leading twist, and provides **better sensitivity to x -dependence of GPDs**.
- ▶ **Proof of factorisation** for this family of processes now available, but intriguing possible violation of collinear factorisation at twist-2 with **gluonic contributions to $\pi^0\gamma$ photoproduction**.
- ▶ **Good statistics** in various experiments, particularly at JLab.

Conclusion

- ▶ Exclusive photoproduction of photon-meson pair provides additional channel for **extracting GPDs**: Interesting effects from choice of different mesons.
- ▶ Especially interesting since it can probe **chiral-odd GPDs** at the leading twist, and provides **better sensitivity to x -dependence of GPDs**.
- ▶ **Proof of factorisation** for this family of processes now available, but intriguing possible violation of collinear factorisation at twist-2 with **gluonic contributions to $\pi^0\gamma$ photoproduction**.
- ▶ **Good statistics** in various experiments, particularly at JLab.
- ▶ **Small ξ limit** of GPDs can be investigated by exploiting high energies available in collider mode such as EIC and UPCs at LHC.

- Understand issues in **gluonic GPD** contributions to

$$\gamma N \rightarrow \gamma \pi^0 N$$

S.N., J. Schönleber, L. Szymanowski, S. Wallon [to appear]

- ▶ Understand issues in **gluonic GPD** contributions to $\gamma N \rightarrow \gamma \pi^0 N$
S.N., J. Schönleber, L. Szymanowski, S. Wallon [to appear]
- ▶ Compute **NLO** corrections (**422** NLO diagrams, vs 20 LO diagrams!). Especially problems with **$i\epsilon$ factors** in rational functions in front of master integrals: [ongoing]

- ▶ Understand issues in **gluonic GPD** contributions to $\gamma N \rightarrow \gamma \pi^0 N$
S.N., J. Schönleber, L. Szymanowski, S. Wallon [to appear]
- ▶ Compute **NLO** corrections (422 NLO diagrams, vs 20 LO diagrams!). Especially problems with **$i\epsilon$ factors** in rational functions in front of master integrals: [ongoing]
- ▶ Generalise to **electroproduction** ($Q^2 \neq 0$).
- ▶ Add **Bethe-Heitler** component (photon emitted from incoming lepton)
 - zero in chiral-odd case.
 - suppressed in chiral-even case.

BACKUP SLIDES

Definition

Quark GPDs: twist 2 Chiral-even

Quark GPDs at twist 2 [Diehl: hep-ph/0307382]

without helicity flip (chiral-even Γ matrices): 4 chiral-even GPDs:
(Note: $\Delta = p' - p$)

$$\begin{aligned} F^q &= \frac{1}{2} \int \frac{dz^-}{2\pi} e^{ixP^+z^-} \langle p' | \bar{q}(-\tfrac{1}{2}z) \gamma^+ q(\tfrac{1}{2}z) | p \rangle \Big|_{z^+=0, z_\perp=0} \\ &= \frac{1}{2P^+} \left[H^q(x, \xi, t) \bar{u}(p') \gamma^+ u(p) + E^q(x, \xi, t) \bar{u}(p') \frac{i \sigma^{+\alpha} \Delta_\alpha}{2m} u(p) \right], \end{aligned}$$

$$\begin{aligned} \tilde{F}^q &= \frac{1}{2} \int \frac{dz^-}{2\pi} e^{ixP^+z^-} \langle p' | \bar{q}(-\tfrac{1}{2}z) \gamma^+ \gamma_5 q(\tfrac{1}{2}z) | p \rangle \Big|_{z^+=0, z_\perp=0} \\ &= \frac{1}{2P^+} \left[\tilde{H}^q(x, \xi, t) \bar{u}(p') \gamma^+ \gamma_5 u(p) + \tilde{E}^q(x, \xi, t) \bar{u}(p') \frac{\gamma_5 \Delta^+}{2m} u(p) \right]. \end{aligned}$$

$H^q \xrightarrow{\xi=0, t=0} \text{PDF } q$

$\tilde{H}^q \xrightarrow{\xi=0, t=0} \text{polarised PDF } \Delta q$

Definition

Quark GPDs: twist 2 Chiral-odd

with helicity flip (chiral-odd Γ matrices): 4 chiral-odd GPDs:

$$\begin{aligned} & \frac{1}{2} \int \frac{dz^-}{2\pi} e^{ixP^+z^-} \langle p' | \bar{q}(-\tfrac{1}{2}z) i \sigma^{+i} q(\tfrac{1}{2}z) | p \rangle \Big|_{z^+=0, z_\perp=0} \\ &= \frac{1}{2P^+} \bar{u}(p') \left[H_T^q i \sigma^{+i} + \tilde{H}_T^q \frac{P^+ \Delta^i - \Delta^+ P^i}{m^2} \right. \\ & \quad \left. + E_T^q \frac{\gamma^+ \Delta^i - \Delta^+ \gamma^i}{2m} + \tilde{E}_T^q \frac{\gamma^+ P^i - P^+ \gamma^i}{m} \right] u(p), \end{aligned}$$

$$H_T^q \xrightarrow{\xi=0, t=0} \text{quark transversity PDFs } \delta q$$

Note: $\tilde{E}_T^q(x, -\xi, t) = -\tilde{E}_T^q(x, \xi, t)$

Why consider a gamma-meson pair?

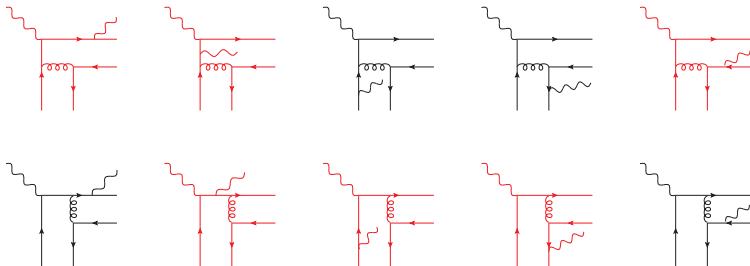
Go to higher twist?

- ▶ Vanishing of chiral-odd amplitude in DVMP only occurs at twist 2
- ▶ At twist 3 this process does not vanish [S. Ahmad, G. Goldstein, S. Liuti: 0805.3568], [S. Goloskokov, P. Kroll: 1106.4897, 1310.1472]
- ▶ However processes involving twist 3 DAs may face problems with factorisation (end-point singularities)

⇒ can be made safe in the high-energy k_T -factorisation approach

[I. Anikin, D. Ivanov, B. Pire, L. Szymanowski, S. Wallon: 0909.4090]

A total of 20 diagrams to compute



- ▶ Need to compute 10 diagrams: Other half related by $q \leftrightarrow \bar{q}$ (anti)symmetry.
- ▶ In fact, by choosing the **right gauge**, **only 4 diagrams** can be used to generate all the others by various symmetries (eg. photon exchange).
- ▶ **Red** diagrams **cancel** in the chiral-odd case

Computation

Parametrising the GPDs: ρ_L and π case, Chiral-even

$$\int \frac{dz^-}{4\pi} e^{ixP^+z^-} \langle p_2, \lambda_2 | \bar{\psi}_q \left(-\frac{1}{2}z^- \right) \gamma^+ \psi \left(\frac{1}{2}z^- \right) | p_1, \lambda_1 \rangle$$
$$= \frac{1}{2P^+} \bar{u}(p_2, \lambda_2) \left[H^q(x, \xi, t) \gamma^+ + E^q(x, \xi, t) \frac{i\sigma^{\alpha+} \Delta_\alpha}{2m} \right] u(p_1, \lambda_1)$$

$$\int \frac{dz^-}{4\pi} e^{ixP^+z^-} \langle p_2, \lambda_2 | \bar{\psi}_q \left(-\frac{1}{2}z^- \right) \gamma^+ \gamma^5 \psi \left(\frac{1}{2}z^- \right) | p_1, \lambda_1 \rangle$$
$$= \frac{1}{2P^+} \bar{u}(p_2, \lambda_2) \left[\tilde{H}^q(x, \xi, t) \gamma^+ \gamma^5 + \tilde{E}^q(x, \xi, t) \frac{\gamma^5 \Delta^+}{2m} \right] u(p_1, \lambda_1)$$

- Take the limit $\Delta_\perp = 0$.
- In that case and for small ξ , the dominant contributions come from H^q and \tilde{H}^q .

Computation

Parametrising the GPDs: ρ_T case, Chiral-odd

$$\begin{aligned} & \int \frac{dz^-}{4\pi} e^{ixP^+z^-} \langle p_2, \lambda_2 | \bar{\psi}_q \left(-\frac{1}{2}z^- \right) i\sigma^{+i} \psi \left(\frac{1}{2}z^- \right) | p_1, \lambda_1 \rangle \\ &= \frac{1}{2P^+} \bar{u}(p_2, \lambda_2) \left[H_T^q(x, \xi, t) i\sigma^{+i} + \tilde{H}_T^q(x, \xi, t) \frac{P^+ \Delta^i - \Delta^+ P^i}{m_N^2} \right. \\ &+ \left. E_T^q(x, \xi, t) \frac{\gamma^+ \Delta^i - \Delta^+ \gamma^i}{2m_N} + \tilde{E}_T^q(x, \xi, t) \frac{\gamma^+ P^i - P^+ \gamma^i}{m_N} \right] u(p_1, \lambda_1) \end{aligned}$$

- Take the limit $\Delta_\perp = 0$.
- In that case and for small ξ , the dominant contributions come from H_T^q .

- ▶ GPDs can be represented in terms of **Double Distributions**

[A. Radyushkin: [hep-ph/9805342](https://arxiv.org/abs/hep-ph/9805342)]

$$H^q(x, \xi, t=0) = \int_{-1}^1 d\beta \int_{-1+|\beta|}^{1-|\beta|} d\alpha \delta(\beta + \xi\alpha - x) f^q(\beta, \alpha)$$

- ▶ ansatz for these Double Distributions:

- ▶ chiral-even sector:

$$\begin{aligned} f^q(\beta, \alpha, t=0) &= \Pi(\beta, \alpha) q(\beta) \Theta(\beta) - \Pi(-\beta, \alpha) \bar{q}(-\beta) \Theta(-\beta), \\ \tilde{f}^q(\beta, \alpha, t=0) &= \Pi(\beta, \alpha) \Delta q(\beta) \Theta(\beta) + \Pi(-\beta, \alpha) \Delta \bar{q}(-\beta) \Theta(-\beta). \end{aligned}$$

- ▶ chiral-odd sector:

$$f_T^q(\beta, \alpha, t=0) = \Pi(\beta, \alpha) \delta q(\beta) \Theta(\beta) - \Pi(-\beta, \alpha) \delta \bar{q}(-\beta) \Theta(-\beta).$$

- ▶ $\Pi(\beta, \alpha) = \frac{3}{4} \frac{(1-\beta)^2 - \alpha^2}{(1-\beta)^3}$: profile function

- simplistic factorised ansatz for the t -dependence:

$$H^q(x, \xi, t) = H^q(x, \xi, t = t_{\min}) \times F_H(t)$$

with $F_H(t) = \frac{(t_{\min} - C)^2}{(t - C)^2}$ a standard **dipole form factor**
($C = 0.71 \text{ GeV}^2$)

Sets of PDFs used to model GPDs

- ▶ $q(x)$: unpolarised PDF:
 - GRV-98 [M. Glück, E. Reya, A. Vogt: hep-ph/9806404]
 - MSTW2008lo [A. Martin, W. Stirling, R. Thorne, G. Watt: 0901.0002]
 - MSTW2008nnlo [A. Martin, W. Stirling, R. Thorne, G. Watt: 0901.0002]
 - ABM11nnlo [S. Alekhin, J. Blumlein, S. Moch: 1202.2281]
 - CT10nnlo [J. Gao, M. Guzzi, J. Huston, H. Lai, Z. Li, P. Nadolsky, J. Pumplin, D. Stump, C.P. Yuan: 1302.6246]
- ▶ $\Delta q(x)$ polarised PDF
 - GRSV-2000 [M. Glück, E. Reya, M. Stratmann, W. Vogelsang: hep-ph/0011215]
- ▶ $\delta q(x)$: transversity PDF:
 - Based on parameterisation for TMDs from which transversity PDFs obtained as limiting case [M. Anselmino, M. Boglione, U. D'Alesio, S. Melis, F. Murgia, A. Prokudin: 1303.3822]

Effects are not significant! But relevant for NLO corrections!

- Helicity conserving (vector) DA at twist 2: ρ_L

$$\langle 0 | \bar{u}(0) \gamma^\mu u(x) | \rho_L^0(p) \rangle = \frac{p^\mu}{\sqrt{2}} f_\rho \int_0^1 du e^{-iup \cdot x} \phi_\rho(u)$$

- Helicity flip (tensor) DA at twist 2: ρ_T

$$\langle 0 | \bar{u}(0) \sigma^{\mu\nu} u(x) | \rho_T^0(p, s) \rangle = \frac{i}{\sqrt{2}} (\epsilon_\rho^\mu p^\nu - \epsilon_\rho^\nu p^\mu) f_\rho^\perp \int_0^1 du e^{-iup \cdot x} \phi_\rho(u)$$

- Helicity conserving (axial) DA at twist 2: π^\pm

$$\langle 0 | \bar{u}(0) \gamma^\mu \gamma^5 d(x) | \pi(p) \rangle = ip^\mu f_\pi \int_0^1 du e^{-iup \cdot x} \phi_\pi(u)$$

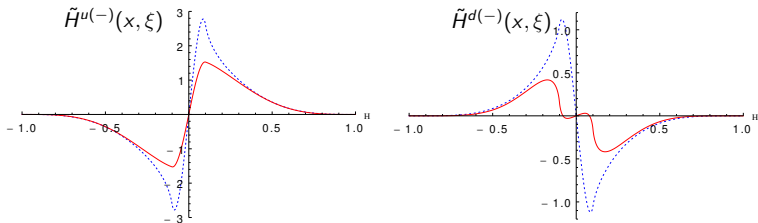
Computation

Valence vs Standard scenarios in \tilde{H} (Chiral-even, Axial)

Typical kinematic point (for JLab kinematics):

$$\xi = .1 \leftrightarrow S_{\gamma N} = 20 \text{ GeV}^2 \text{ and } M_{\gamma\rho}^2 = 3.5 \text{ GeV}^2$$

$$\tilde{H}^{q(-)}(x, \xi, t) = \tilde{H}^q(x, \xi, t) - \tilde{H}^q(-x, \xi, t) \quad [C = -1]$$



“valence” and “standard”: two GRSV Ansätze for $\Delta q(x)$

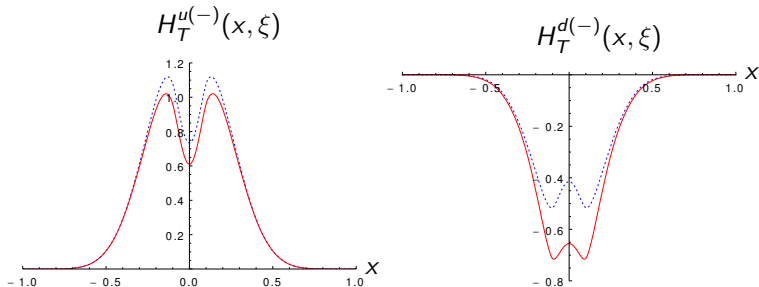
Computation

Valence vs Standard scenarios in H_T (Chiral-odd)

Typical kinematic point (for JLab kinematics):

$$\xi = .1 \leftrightarrow S_{\gamma N} = 20 \text{ GeV}^2 \text{ and } M_{\gamma\rho}^2 = 3.5 \text{ GeV}^2$$

$$H_T^{q(-)}(x, \xi, t) = H_T^q(x, \xi, t) + H_T^q(-x, \xi, t) \quad [C = -1]$$



“valence” and “standard”: two GRSV Ansätze for $\Delta q(x)$

\Rightarrow two Ansätze for $\delta q(x)$

Kinematics

- Work in the limit of:

- $\Delta_{\perp} \ll p_{\perp}$
- $m_N^2, m_M^2 \ll M_{\gamma M}^2$

- initial state particle momenta:

$$q^\mu = n^\mu,$$

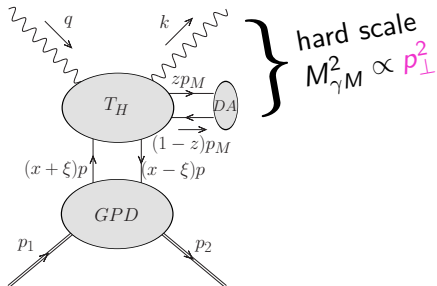
$$p_1^\mu = (1 + \xi) p^\mu + \frac{m_N^2}{s(1+\xi)} n^\mu$$

- final state particle momenta:

$$p_2^\mu = (1 - \xi) p^\mu + \frac{m_N^2 + \vec{p}_t^2}{s(1 - \xi)} n^\mu + \Delta_\perp^\mu$$

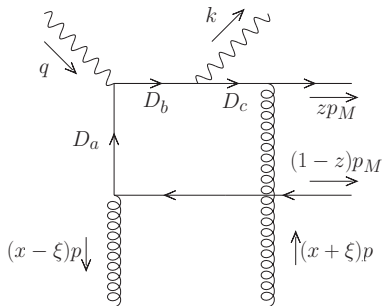
$$k^\mu = \alpha \textcolor{red}{n}^\mu + \frac{(\vec{p}_t - \vec{\Delta}_t/2)^2}{\alpha s} p^\mu + \textcolor{violet}{p}_\perp^\mu - \frac{\Delta_\perp^\mu}{2}, \quad \Delta \downarrow$$

$$p_M^\mu = \alpha_M \textcolor{red}{n}^\mu + \frac{(\vec{p}_t + \vec{\Delta}_t/2)^2 + m_M^2}{\alpha_M s} p^\mu - \textcolor{violet}{p}_\perp^\mu - \frac{\Delta_\perp^\mu}{2},$$



Exclusive photoproduction of $\pi^0\gamma$

Gluonic GPD contributions



$$D_a = ((x - \xi)p + \bar{z}p_M)^2 + i\epsilon$$

$$= s\bar{\alpha}\bar{z}[x - \xi + i\epsilon] ,$$

$$D_b = (k + zp_M - (x + \xi)p)^2 + i\epsilon$$

$$= -s[z(x - \xi - i\epsilon) + \alpha\bar{z}(x + \xi - i\epsilon)] ,$$

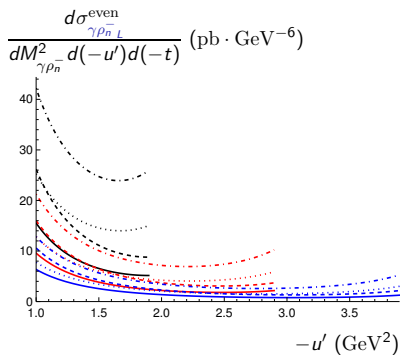
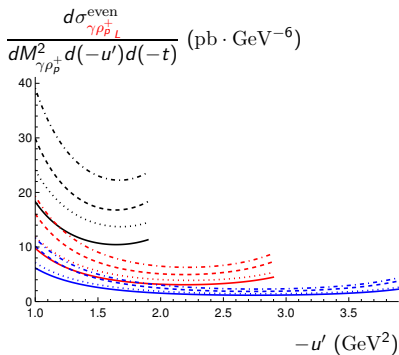
$$D_c = (zp_M - (x + \xi)p)^2 + i\epsilon$$

$$= -s\bar{\alpha}z[x + \xi - i\epsilon]$$

\Rightarrow *pinching of poles in the propagators (D_a and D_b) in the limit of $z \rightarrow 1$*

Results

Fully-differential cross-sections: $\gamma\rho_P^+_L$ vs $\gamma\rho_N^-_L$



$$S_{\gamma N} = 20 \text{ GeV}^2, -t = (-t)_{\min}, M_{\gamma\rho}^2 = 3, 4, 5 \text{ GeV}^2$$

Dashed: Holographic DA non-dashed: Asymptotical DA

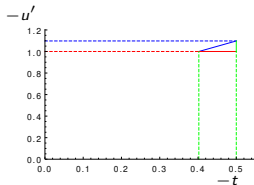
Dotted: standard scenario non-dotted: valence scenario

Results

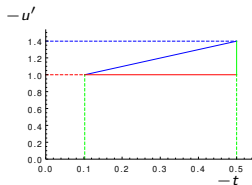
Phase space integration: Evolution in $(-t, -u')$ plane

large angle scattering: $M_{\gamma\rho}^2 \sim -u' \sim -t'$ ($S_{\gamma N} = 20 \text{ GeV}^2$)

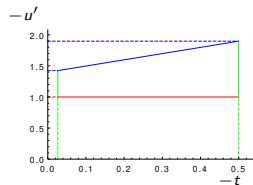
$\Rightarrow -u' > 1 \text{ GeV}^2$ and $-t' > 1 \text{ GeV}^2$ and $(-t)_{\min} \leq -t \leq .5 \text{ GeV}^2$



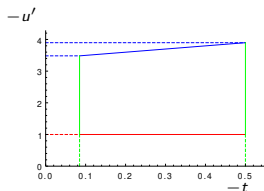
$M_{\gamma\rho} = 2.2 \text{ GeV}^2$



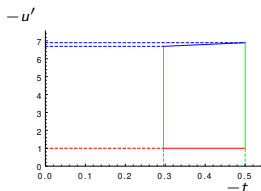
$M_{\gamma\rho} = 2.5 \text{ GeV}^2$



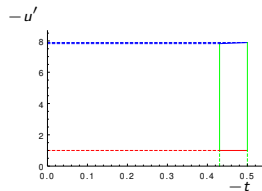
$M_{\gamma\rho} = 3 \text{ GeV}^2$



$M_{\gamma\rho} = 5 \text{ GeV}^2$



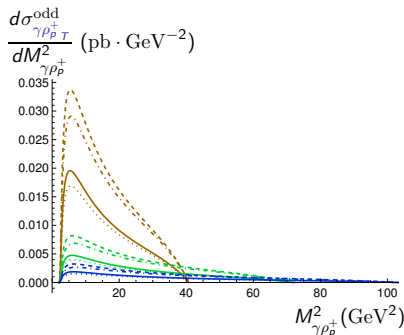
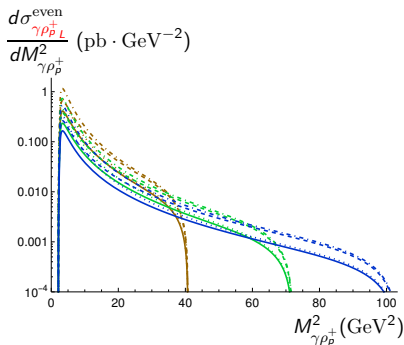
$M_{\gamma\rho} = 8 \text{ GeV}^2$



$M_{\gamma\rho} = 9 \text{ GeV}^2$

Results

Single differential cross-section: $\gamma\rho_{pL}^+$ vs $\gamma\rho_{pT}^+$



$$S_{\gamma N} = 80, 140, 200 \text{ GeV}^2$$

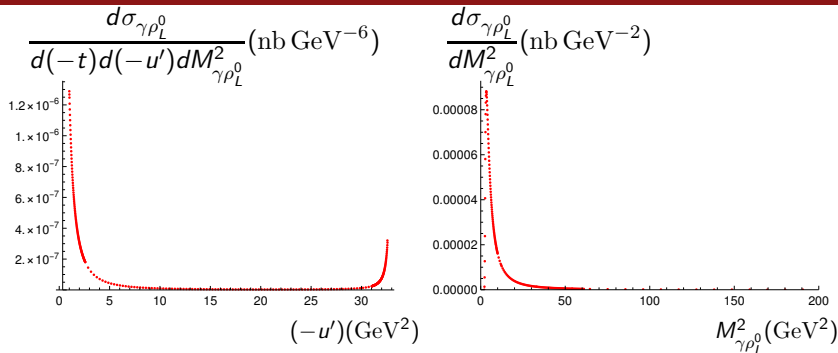
Dashed: Holographic DA non-dashed: Asymptotical DA

Dotted: standard scenario non-dotted: valence scenario

⇒ CO cross-section is suppressed by a factor of ξ^2 ($\xi \approx \frac{M_{\gamma\rho}^2}{2S_{\gamma N}}$):
Measurable at small $S_{\gamma N}$, but drops rapidly with increasing $S_{\gamma N}$.

Results

Necessity for Importance Sampling



- ▶ Need enough points at boundaries for distribution in $(-u')$
- ▶ Need enough points to resolve peak (at low $M_{\gamma\rho_L^0}^2$) for distribution in $M_{\gamma\rho_L^0}^2$

Results

Explaining the difference between chiral-even and chiral-odd plots

► $\xi = \frac{M_{\gamma M}^2}{2S_{\gamma N} - M_N^2} \approx \frac{M_{\gamma M}^2}{2S_{\gamma N}}$ for $M_{\gamma M}^2 \ll S_{\gamma N}$

► Chiral-even (unpolarised) cross-section:

$$|\overline{\mathcal{M}}_{\text{CE}}|^2 = \frac{2}{s^2}(1 - \xi^2)C_{\text{CE}}^2 \left\{ 2|N_A|^2 + \frac{p_{\perp}^4}{s^2}|N_B|^2 + \frac{p_{\perp}^2}{s}(N_A N_B^* + \text{c.c.}) + \frac{p_{\perp}^4}{4s^2}|N_{A_5}|^2 + \frac{p_{\perp}^4}{4s^2}|N_{B_5}|^2 \right\}.$$

► Chiral-odd (unpolarised) cross-section:

$$|\overline{\mathcal{M}}_{\text{CO}}|^2 = \frac{2048}{s^2}\xi^2(1 - \xi^2)C_{\text{CO}}^2 \left\{ \alpha^4 |N_{TA}|^2 + |N_{TB}|^2 \right\}.$$

► Note: $\alpha = \frac{-u'}{M_{\gamma M}^2}$.

Results

Integrated cross-section: Mapping procedure for different values of $S_{\gamma N}$

To obtain distribution in $S_{\gamma N}$, we exploit non-trivial mapping between 1 set of data at a fixed $S_{\gamma N}$ to other values $\tilde{S}_{\gamma N}$ *lower* than it.

$$\tilde{M}_{\gamma M}^2 = M_{\gamma M}^2 \frac{\tilde{S}_{\gamma N} - m_N^2}{S_{\gamma N} - m_N^2},$$
$$- \tilde{u}' = \frac{\tilde{M}_{\gamma M}^2}{M_{\gamma M}^2} (-u').$$

Implementing *importance sampling* \implies careful consideration of the various limits involved are needed.

Mapping possible since *different* sets of $(S_{\gamma N}, M_{\gamma M}^2, -u')$ correspond to the *same* (α, ξ) .

$$\alpha = \frac{-u'}{M_{\gamma M}^2}, \quad \xi = \frac{M_{\gamma M}^2}{2(S_{\gamma N} - m_N^2) - M_{\gamma M}^2}.$$

Results

Why does the circular asymmetry vanish for unpolarised target?

Consider

$$\gamma(q, \lambda_q) + N(p_1, \lambda_1) \rightarrow \gamma(k, \lambda_k) + \pi^\pm(p_\pi) + N'(p_2, \lambda_2) ,$$

where λ_i represent the helicities of the particles.

QED/QCD **invariance under parity** implies that [C. Bourrely, J. Soffer, E. Leader: Phys.Rept. 59 (1980) 95-297]

$$\mathcal{A}_{\lambda_2 \lambda_k ; \lambda_1 \lambda_q} = \eta (-1)^{\lambda_1 - \lambda_q - (\lambda_2 - \lambda_k)} \mathcal{A}_{-\lambda_2 - \lambda_k ; -\lambda_1 - \lambda_q} ,$$

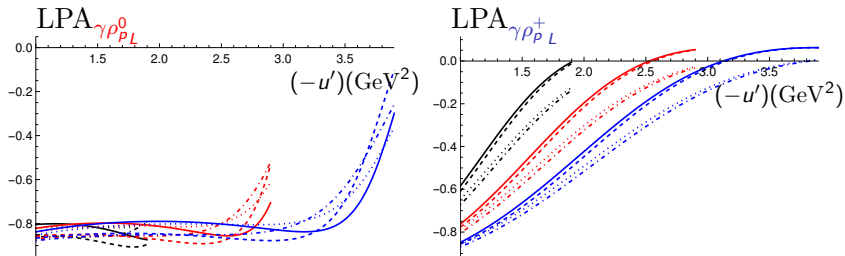
where η represents phase factors related to intrinsic spin.

Thus, at the cross-section level, it is clear that circular asymmetry will vanish, since

$$\sum_{\lambda_i, i \neq q} |\mathcal{A}_{\lambda_2 \lambda_k ; \lambda_1 +}|^2 = \sum_{\lambda_i, i \neq q} |\mathcal{A}_{\lambda_2 \lambda_k ; \lambda_1 -}|^2$$

Results

LPA wrt incoming photon: Fully-differential level: $\gamma\rho_{pL}^0$ vs $\gamma\rho_{pL}^+$



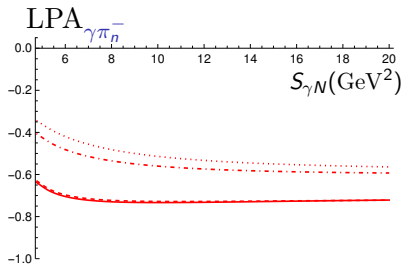
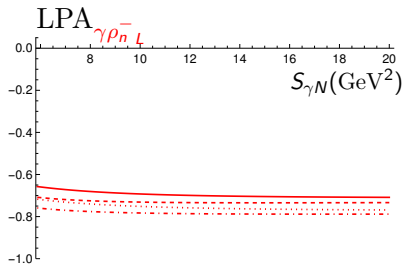
$$S_{\gamma N} = 20 \text{ GeV}^2, -t = (-t)_{\min}, M_{\gamma\rho}^2 = 3, 4, 5 \text{ GeV}^2$$

Dashed: Holographic DA non-dashed: Asymptotical DA

Dotted: standard scenario non-dotted: valence scenario

Results

LPA wrt incoming photon: Integrated level: $\gamma\rho_n^-$ vs $\gamma\pi_n^-$



Dashed: Holographic DA

non-dashed: Asymptotical DA

Dotted: standard scenario

non-dotted: valence scenario

⇒ LPAs are sizeable!

At COMPASS:

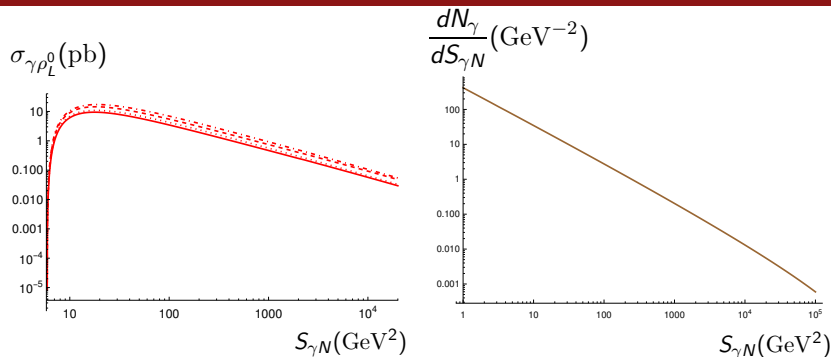
- ▶ Taking a luminosity of $\mathcal{L} = 0.1 \text{ nb}^{-1}\text{s}^{-1}$, and 300 days of run,
 - ρ_L^0 (on p) : $\approx 1.2 \times 10^3$
 - ρ_T^0 (on p) : $\approx 1.5 \times 10^2$ (Chiral-odd)
 - ρ_L^+ : $\approx 7.4 \times 10^2$
 - ρ_T^+ : $\approx 2.6 \times 10^2$ (Chiral-odd)
 - π^+ : $\approx 7.4 \times 10^2$
- ▶ Lower numbers due to low luminosity (factor of 10^3 less than JLab!)

For p-Pb UPCs at LHC (integrated luminosity of 1200 nb^{-1}):

- ▶ With future data from runs 3 and 4,
 - $\rho_L^0 : \approx 1.6 \times 10^4$
 - $\rho_T^0 : \approx 1.7 \times 10^3$ (Chiral-odd)
 - $\rho_L^+ : \approx 1.1 \times 10^4$
 - $\rho_T^+ : \approx 2.9 \times 10^3$ (Chiral-odd)
 - $\pi^+ : \approx 9.3 \times 10^3$
- ▶ $300 < S_{\gamma N} / \text{GeV}^2 < 20000$ ($5 \cdot 10^{-5} < \xi < 5 \cdot 10^{-3}$):
 - $\rho_L^0 : \approx 8.1 \times 10^2$
 - $\rho_L^+ : \approx 6.4 \times 10^2$
 - $\pi^+ : \approx 3.4 \times 10^2$

Prospects at experiments

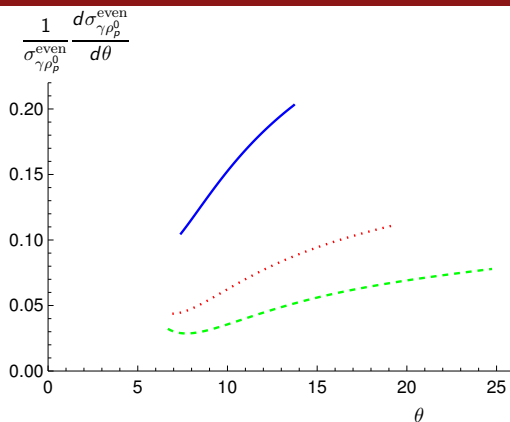
Why counting rates not as high for UPCs at LHC?



- ▶ Photon flux enhanced by a factor of Z^2 , but drops rapidly with $S_{\gamma N} \implies$ *Low luminosity not compensated by larger photon flux.*
- ▶ LHC great for high energy, but JLab better in terms of luminosity.
- ▶ Still, LHC gives us access to the small ξ region of GPDs!

Angular cuts on outgoing photon at JLab

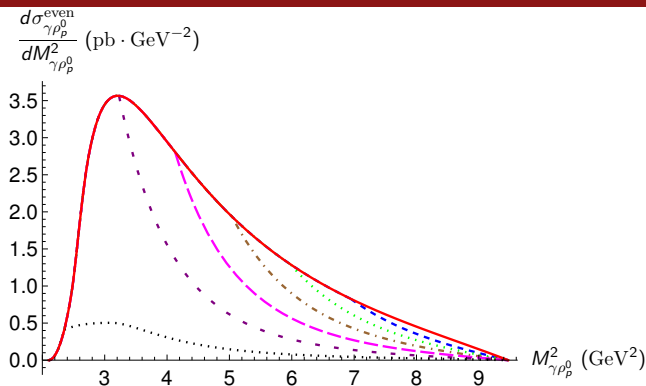
Angular distribution: $\rho_p^0 \gamma$ photoproduction at $S_{\gamma N} = 20 \text{ GeV}^2$



- $M_{\gamma\rho_p^0}^2 = 4 \text{ GeV}^2$ (solid blue)
- $M_{\gamma\rho_p^0}^2 = 6 \text{ GeV}^2$ (dotted red)
- $M_{\gamma\rho_p^0}^2 = 8 \text{ GeV}^2$ (dashed green)

Angular cuts on outgoing photon at JLab

Single differential cross-section: $\rho_p^0 \gamma$ photoproduction at $S_{\gamma N} = 20 \text{ GeV}^2$



- ▶ no angular cut (solid red)
- ▶ $\theta \leq 35^\circ$ (dashed blue)
- ▶ $\theta \leq 30^\circ$ (dotted green)
- ▶ $\theta \leq 25^\circ$ (dashed-dotted brown)
- ▶ $\theta \leq 20^\circ$ (long-dashed magenta)
- ▶ $\theta \leq 15^\circ$ (short-dashed purple)
- ▶ $\theta \leq 10^\circ$ (dotted black)